

Synthesis of One-Dimensional and Porous TiO₂ Nanostructures by Controlled Hydrolysis of Titanium Alkoxide via Coupling with an Esterification Reaction

Ziyi Zhong,^{*,†} Thiam-Peng Ang,[†] Jizhong Luo,[†] Hwee-Chin Gan,[†] and Aharon Gedanken^{*,‡}

Institute of Chemical Engineering and Sciences, 1 Pesek Road, Jurong Island, Singapore 627833, and Department of Chemistry and Kanbar Laboratory for Nanomaterials, Bar-Ilan University Center for Advanced Materials and Nanotechnology, Bar-Ilan University, Ramat-Gan 52900, Israel

Received July 31, 2005. Revised Manuscript Received October 9, 2005

1-Dimensional (1-D) TiO₂ nanostructures were prepared by a novel one-pot method, in which the water release was controlled by an esterification reaction between acetic acid and 2-propanol, and the alkoxide was partially coordinated with carboxylic acid, thus the hydrolysis step was significantly slowed. The successive unidirectional growth of TiO₂ nanostructures was realized by using aniline, octylamine, and isobutylamine, respectively, as structure-directing agents. After calcination below 400 °C, 1-D and porous nanostructures of TiO₂ anatase were obtained. Preliminary results showed that Au supported on these TiO₂ nanofibers, compared with catalyst using commercial TiO₂ as support, has much higher catalytic activity for CO oxidation at near ambient temperature.

Introduction

TiO₂ is primarily an industrial pigment in paints but has various other applications in research, e.g., as a photocatalyst,¹ a heterogeneous catalyst support,² in sensor devices,³ ductile ceramics,⁴ and as a possible H₂-storage material.⁵ The properties and performance of TiO₂ often depends on its crystalline phase state, dimensions, and morphology.⁶ In photocatalysis, low quantum yields are observed for spherical nanocrystals of TiO₂; below 10 nm in size due to a significant increased opportunity for bulk recombination among electrons (e⁻) and holes (h⁺).⁷ In 1-dimensional (1-D) nanorods of TiO₂, the surface-to-volume ratio is typically higher than in spherical TiO₂ of similar size. As a result, a higher density of active sites for photocatalysis and a higher interfacial charge carrier transfer rate are possible.⁸ However, the search for an one-pot synthesis of nanosized TiO₂ with well-controlled size and shape is still a big challenge.

1-D nanostructures (wires, rods, and tubes) have become the focus of intensive research in recent years⁹ because of

their unique thermal, optical, and mechanical properties that are different from those of the bulk particles or extended forms¹⁰ and their application in nanodevice fabrication.¹¹ Existing methods to synthesize 1-D TiO₂ nanostructures mainly comprise template,¹² alkali treated hydrothermal reaction between NaOH and TiO₂,¹³ and surfactant-directed methods.¹⁴ The alkali treatment under hydrothermal conditions results in the formation of TiO₂ nanotubes, while the surfactant-directed synthesis usually leads to the formation of ellipsoidal anatase with relatively low aspect ratio.¹⁴ Although the possibility to “fine tune” the morphology of 1-D TiO₂ nanostructures during synthesis is a highly desirable goal, successes have been rare, unlike the case of silica. The prime difficulty is that titanium precursors hydrolyze too fast; thus the nucleation and growth steps are not well separated.¹⁵

One strategy to lower the hydrolysis rate of Ti alkoxides is to form titanium complexes by ligand exchange reaction, e.g., using oleic acid¹⁶ and glycols¹⁷ to replace the alcoholic groups. In such rare examples, spherical TiO₂ particles¹⁵ were

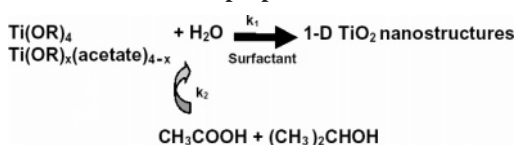
* Corresponding authors. E-mail: zhong_ziyi@ices.a-star.edu.sg (Z.Z.); gedanken@mail.biu.ac.il (A.G.).

[†] Institute of Chemical Engineering and Sciences.

[‡] Bar-Ilan University.

- (1) (a) Pelizzetti, E.; Serpone, N., Eds. *Photocatalysis: Fundamentals and Applications*; Wiley: New York, 1989. (b) Wang, X. C.; Yu, J. C.; Yip, H. Y.; Wu, L.; Wong, P. K.; Lai, S. Y. *Chem.—Eur. J.* **2005**, *11*, 2997.
- (2) (a) Haruta, M.; Yamada, N.; Kobayashi, T.; Iijima, S. *J. Catal.* **1989**, *115*, 301. (b) Valden, M.; Lai, X.; Goodman, D. W. *Science* **1998**, *281*, 1647.
- (3) (a) Wang, R.; Hashimoto, K.; Fijishima, A. *Nature* **1997**, *388*, 431. (b) Traveria, E.; Gnappi, G.; Monternero, A.; Gusmano, G. *Sens. Actuators, B* **1996**, *31*(1–2), 59.
- (4) Karch, J.; Barringer, R.; Gleiter, H. *Nature* **1987**, *330*, 556.
- (5) Lim, S. H.; Luo, J.; Zhong, Z. Y.; Ji, W.; Lin, J. *Inorg. Chem.* **2005**, *44*, 12, 4124.
- (6) Melendres, C. A.; Narayanasamy, A.; Maroni, V. A.; Siegel, R. W. *J. Mater. Res.* **1989**, *4*, 1246.
- (7) Zhang, Z.; Wang, C. C.; Zakaria, R.; Ying, J. Y. *J. Phys. Chem. B* **1998**, *102*, 10871.
- (8) Manna, L.; Scher, E. C.; Li, L. S.; Alivisatos, A. P. *J. Am. Chem. Soc.* **2002**, *124*, 7136.
- (9) (a) Xia, Y.; Yang, P.; Sun, Y.; Wu, Y.; Mayers, B.; Gates, B.; Yin, Y.; Kim, F.; Yan, H. *Adv. Mater.* **2003**, *15*(5), 353. (b) Zhong, Z. Y.; Luo, J.; Ang, T. P.; Highfield, J. G.; Lin, J.; Gedanken, A. *J. Phys. Chem. B* **2004**, *108*, 18119–18223.
- (10) Feldheim, D. *The Electrochemical Society Interface Fall Meeting* **2001**, 22–25.
- (11) (a) Anelli, P. L.; Spencer, N.; Stoddart, J. F. *J. Am. Chem. Soc.* **1991**, *113*, 5131. (b) Whites, G. M.; Love, J. C. *Sci. Am.* **2001**, 33–41. (c) Alivisatos, A. P.; Barbara, P. F.; Castleman, A. W.; Chang, J.; Dixon, D. A.; Klein, M. L.; McLendon, G. L.; Miller, J. S.; Ratner, M. A.; Rossky, P.; Stupp, S.; Thompson, M. E. *Adv. Mater.* **1998**, *10*, 1297–1336.
- (12) (a) Martin, C. R. *Science* **1994**, *266*, 1961. (b) Hoyer, P. *Langmuir* **1996**, *12*, 1411. (c) Zhong, Z. Y.; Yin, Y.; Gates, B.; Xia, Y. *Adv. Mater.* **2000**, *12*, 206–209.
- (13) (a) Kasuga, T.; Hiramatsu, M.; Hoson, A.; Sekino, T.; Niihara, K. *Langmuir* **1998**, *14*, 3160. (b) Kasuga, T.; Hiramatsu, M.; Hoson, A.; Sekino, T.; Niihara, K. *Adv. Mater.* **1999**, *11*(15), 1307. (c) Zhu, Y.; Li, H.; Koltypin, Y.; Hacoben, Y. R.; Gedanken, A. *Chem. Comm.* **2001**, 2616.
- (14) (a) Chemseddine, A.; Moritz, T. *Eur. J. Inorg. Chem.* **1999**, 235. (b) Kanic, K.; Sugimoto, T. *Chem. Commun.* **2004**, 1584. (c) Sugimoto, T.; Okada, K.; Itoh, H. *J. Colloid Interface Sci.* **1997**, 193.
- (15) Jiang, X.; Herricks, T.; Xia, Y. *Adv. Mater.* **2003**, *15*(12), 1205.

Scheme 1. Controlled Hydrolysis of TTIP Realized by Supplying the Water Indirectly from the In Situ Esterification Reaction between Acetic Acid and Isopropanol^a



^a Alkylamines and aniline are used as structure-directing reagents (surfactants) to promote the formation of 1-D nanostructured TiO₂.

obtained in the absence of surfactants, and TiO₂ nanorods with relatively low aspect ratio were observed in the presence of tertiary amines or quaternary ammonium hydroxides.¹⁶ Sugimoto et al.^{14b,c} developed a two-step sol–gel process for synthesis of ellipsoid and cube forms of TiO₂. In the first stage, a rigid gel containing the Ti(TEOA) complex (TEOA = triethanolamine) and a “shape controller” (ammonia) was formed. Subsequent aging at a higher temperature was employed to encourage nucleation and growth of particles. Cozzoli et al.¹⁶ were able to tune the hydrolysis rate of Ti alkoxide, supplying water slowly via the esterification reaction of oleic acid and ethyleneglycol, but they failed to obtain any 1-D TiO₂ structures though three kind of organic amines (trimethylamino-*N*-oxide, triethylamine, and triethylamine) were used.

By consideration of the fact that hydrolysis of Ti alkoxides is inherently fast, the issue of water supply becomes relatively straightforward. In this study, we report the formation of 1-D and porous TiO₂ nanostructures by coupling the hydrolysis to an esterification reaction between acetic acid and 2-propanol (Scheme 1). To obtain these rodlike nanostructures, alkylamines and aniline were added as surfactants to promote unidirectional growth. These primary alkylamines are good structure-directing agents for the formation of 1-D structures of VO_x and Mg(OH)₂¹⁸ but never succeeded in the TiO₂ case, probably because of the very fast hydrolysis of Ti alkoxides. In addition, we proved previously that these primary alkylamines can lead to the formation of meso-pores in TiO₂.¹⁹ Thus, the combination of controlled hydrolysis reaction and directed-growth can lead to the formation of TiO₂ possessing both 1-D and porous structures. To our knowledge, this is the first one-spot synthesis of TiO₂ with such structures.

Experimental Section

All chemicals were of high purity and used as received. Acetic acid (>99.99%), titanium tetraisopropoxide (TTIP), aniline, octylamine, and isobutylamine were purchased from Aldrich and stored in a glovebox. In a typical synthesis, 30 mL of high purity acetic acid was put in a screw-capped autoclave containing a Teflon vessel. TTIP (1 mmol) was dissolved in 3 mL of 2-propanol under stirring until a transparent solution was observed. Then the TTIP solution

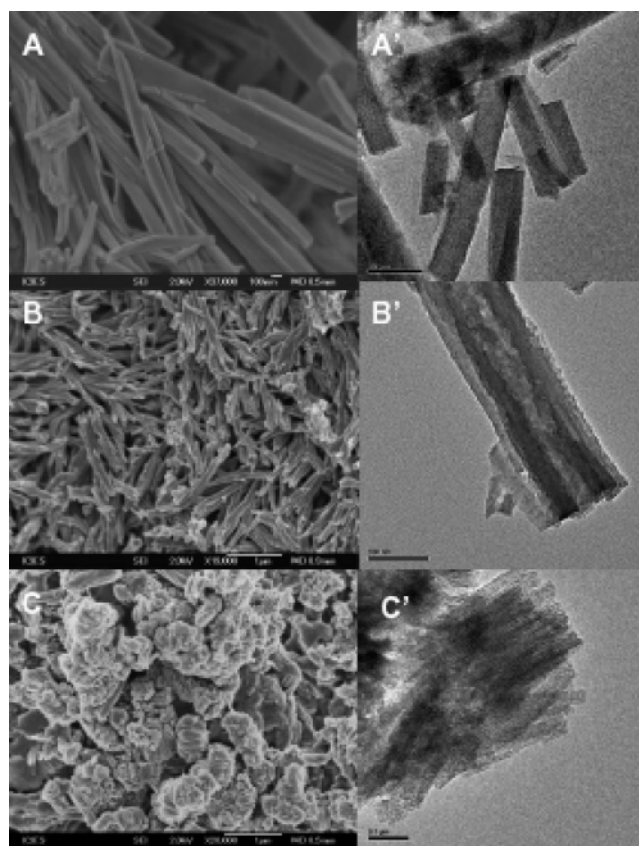


Figure 1. Electronic microscopy images of the as-prepared 1-D TiO₂ nanostructures. A, B, and C are SEM images of the TiO₂ product from aniline (AL), octylamine (OLA), and isobutylamine (IBA) as structure-directing reagents, respectively. A', B', and C' are the corresponding TEM images. The molar ratio of acetic acid:2-propanol:TTIP:surfactant is 400:40:1:1. The three preparations are denoted as TiO₂-AL, TiO₂-OLA, and TiO₂-IBA, respectively.

was transferred to the Teflon vessel, and 1.0 mmol of the respective alkylamine was added. Finally, one drop of H₂SO₄ was added as catalyst to accelerate the esterification reaction. The mixture was purged with N₂, and the autoclave was held at 100 °C for 3–4 h. After reaction, the precipitate was washed with acetone or anhydrous ethanol and dried in a vacuum oven at 100 °C.

The Au loading in the Au/TiO₂ catalyst was ca. 1.0%. The measurement of catalytic oxidation of CO was carried out in a fixed-bed microreactor. Prior to testing, the catalyst was pretreated in air at 200 °C for 1 h. Reactant gas containing 1% CO in air was passed through the catalyst bed at a gas hourly space velocity (GHSV) of 15 000 h⁻¹. The outlet gases were analyzed with an on-line gas chromatography (GC) (Shimadzu) equipped with one thermal conductivity detector and one flame ionization detector.

The shape and size of the TiO₂ samples (and the Au/TiO₂ catalyst) were observed on a transmission electron microscope (TEM, Tecnai TF20 Super Twin, 200 kV) and scanning electron microscope (SEM, JEOL-6700F). The powder X-ray diffraction (XRD) analysis was conducted on a Bruker D8 Advance X-ray diffractometer with Cu Kα₁ radiation, while the thermal analysis (TGA) was performed on a SDT 2960 instrument in air flow. The surface area was measured at 77K (liquid nitrogen) on a Quantachrome Autosorb-6B Surface Area & Pore Size Analyzer. The TiO₂ fibers were calcined at 300 °C for 2 h with a heating rate of 2 °C/min prior to the measurement. The average pore size and surface area were determined based on the Brunauer–Emmett–Teller (BET) model of adsorption.

Results and Discussion

Figure 1 shows the SEM and TEM images of the 1-D TiO₂ intermediate nanostructures. When aniline (AL) was used

- (16) Cozzoli, P. D.; Kornowski, A.; Weller, H. *J. Am. Chem. Soc.* **2003**, *125*, 14539.
- (17) Puri, D. M.; Mehrotra, R. C. *Ind. J. Chem.* **1967**, *51*, 448.
- (18) (a) Li, Y.; Sui, M.; Ding, Y.; Zhang, G.; Zhuang, J.; Wang, C. *Adv. Mater.* **2000**, *12*, 9818. (b) Muhr, H. J.; Krumeich, F.; Schonholzer, U. P.; Bieri, F.; Niederberger, M.; Gauckler, L. J.; Nesper, R. *Adv. Mater.* **2000**, *12*(3), 231. (c) Fric, H.; Schubert, U. *New. J. Chem.* **2005**, *29*, 232–236.
- (19) (a) Wang, Y.; Tang, X.; Yin, L.; Huang, W.; Hachoen, Y. R.; Gedanken, A. *Adv. Mater.* **2000**, *12*(16), 1183. (b) Perkas, N.; Wang, Y.; Koltypin, Y.; Gedanken, A.; Chandrasekaran, S. *Chem. Commun.* **2001**, 988.

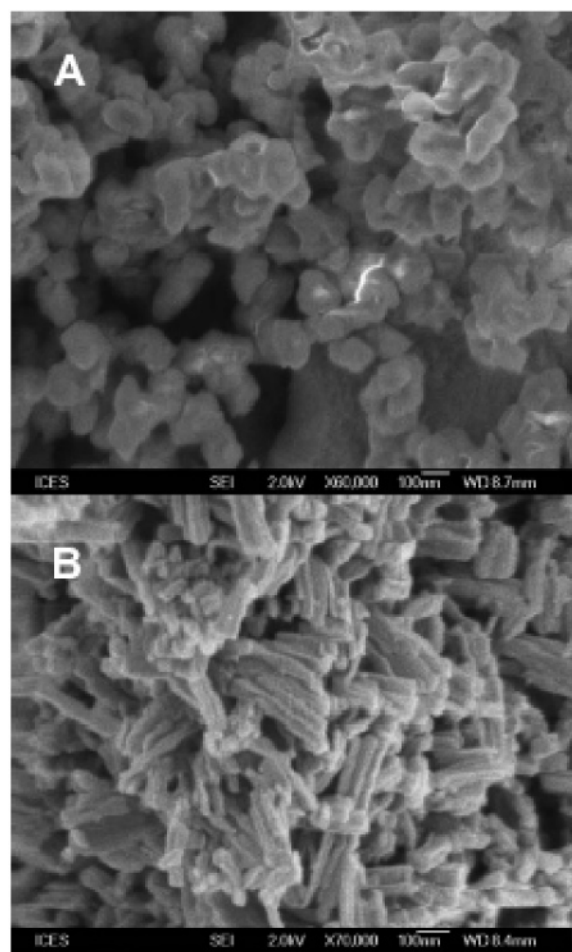


Figure 2. Influence of OLA/Ti ratio on the texture of the TiO_2 product. OLA/Ti = 0:1 (A) and 2:1 (B).

as a surfactant, fibers with cross sections in the range 40–150 nm, and lengths from 150 nm to 3 μm , were obtained (aspect ratio = 4–30). These TiO_2 fibers are remarkably straight and appear of quite smooth surface texture (parts A and A' of Figure 1). This TiO_2 intermediate is denoted as $\text{TiO}_2\text{-AL}$. When octylamine (OLA) was used as a surfactant, fibers were still obtained (parts B and B' of Figure 1), but of somewhat larger diameters (70–100 nm) and with a shorter aspect ratio (~ 10). Fibers appear bundled together, more tubular (with tips “uncapped”), and with rougher surfaces (Figure 1B'). This TiO_2 intermediate is denoted as $\text{TiO}_2\text{-OLA}$. In the case of isobutylamine (IBL), very short TiO_2 fibers were obtained (parts C and C' of Figure 1). Both the diameter (20–30 nm) and the length of these fibers (100–200 nm) are lower relative to the use of other surfactants, and the aspect ratio is just 3–7 (this TiO_2 intermediate is denoted as $\text{TiO}_2\text{-IBA}$). Many of these short fibers are clustered together, each group resembling the florets of a cauliflower. However, upon subsection to strong ultrasonic irradiation, these florets can be dispersed (Figure 4D), indicating that these fibers are loosely packed. As is the case for single-walled five-carbon nanotubes, probably only weak van der Waals forces are responsible for the bundling effect.

The crucial roles of rate-controlled water release, and the presence of surfactants, in promoting the formation of 1-D TiO_2 nanostructures were demonstrated as follows. Prior addition of various trace levels of water in the presence of the

above-mentioned organic amines (molar ratios of TTIP: H_2O = 1:0.1, 1:0.2, 1:0.6, and 1:1, respectively), or in the absence of the organic amines but without previous water addition, did not lead to the formation of any TiO_2 fibers (Figure 2A). However, increase of the molar ratio surfactant:TTIP did have a slight influence on the morphology and size of the TiO_2 nanostructures, as shown for octylamine in Figure 2B.

Actually the synthesized 1-D nanostructures of TiO_2 intermediate are in a precursor form and contain copious levels of H_2O and organic ligands. TG analysis result showed that, for $\text{TiO}_2\text{-OLA}$ (TGA curve is not shown here), upon heating to 400 $^\circ\text{C}$ in flowing air, the weight loss attained for $\text{TiO}_2\text{-OLA}$ was 46.8%. In the differential scanning calorimetry (DSC) curve, there are two sharp peaks located at 343.6 and 431.4 $^\circ\text{C}$, respectively. The huge peak in the range of 300–400 $^\circ\text{C}$ should be attributed to conversion from titanate to TiO_2 anatase and the decomposition of organics. As XRD shows that the as-prepared $\text{TiO}_2\text{-OLA}$ is only poorly crystalline (Figure 3B, bottom trace). After heating at 400 $^\circ\text{C}$ for 3 h, reflections of the anatase phase develop (Figure 3B, upper line), and the calculated thickness for TiO_2 nanocrystals along the (101) reflection is 10.6 nm. Similar results were observed for $\text{TiO}_2\text{-AL}$ and $\text{TiO}_2\text{-IBA}$. Elsewhere, for titanate nanotubes prepared by hydrothermal treatment, Armstrong et al.²⁰ observed the conversion from titanate to TiO_2 (anatase) nanotubes below 400 $^\circ\text{C}$. In the DSC curve (Figure 3A), a huge endothermic peak in the range of 500–750 $^\circ\text{C}$ is observed. XRD results confirmed that the sample calcined at 500 and 600 $^\circ\text{C}$ are still anatase, but the samples calcined at 800 $^\circ\text{C}$ develops rutile peaks, so the transition temperature from anatase to rutile should be between 600–800 $^\circ\text{C}$ (identified by XRD but its pattern is not shown here).

The 1-D TiO_2 nanostructures exhibited different stability under calcination. For $\text{TiO}_2\text{-AL}$, the 1-D nanostructure was retained after calcination at 300 $^\circ\text{C}$ but partially collapsed after 400 $^\circ\text{C}$ treatment (parts A and B of Figure 4). High-temperature calcination removed all of the H_2O and organic ligands. Figure 4A shows the skeletal shape of the residual fibers, while a magnified region in Figure 4B reveals two zones with different lattice orientation (marked with arrows). This “pearl-necklace” pattern suggests that the original 1-D structure consisted in some degree of agglomerates. For $\text{TiO}_2\text{-OLA}$ (Figure 4C) and $\text{TiO}_2\text{-IBA}$ (Figure 4D), the structures are stable up to 400 $^\circ\text{C}$ but collapsed after calcination at 600 $^\circ\text{C}$ for 2 h (Figure 4F). Clearly, the 1-D structures are less thermally stable than the spherical structures. Unlike $\text{TiO}_2\text{-AL}$ (Figure 4A) and $\text{TiO}_2\text{-IBA}$ (Figure 4D), $\text{TiO}_2\text{-OLA}$ (parts C and E of Figure 4) appears substantially porous with an outer wall thickness of about 3–5 nm. The surface area for $\text{TiO}_2\text{-OLA}$ is about 273 and 223 m^2/g after calcination at 300 and 400 $^\circ\text{C}$, respectively. The isotherm of adsorption and desorption is shown in Figure 5, revealing the porous structure of TiO_2 after calcination.

The formation mechanism of the 1-D TiO_2 structures is still not very clear. The observation of 1-D TiO_2 structures

(20) Armstrong, A. R.; Armstrong, G.; Canales, J.; Bruce, P. G. *Angew. Chem., Int. Ed.* **2004**, 43, 2286.

(21) Chandler, D. C.; Roger, M. J.; Mark, J. *Chem. Rev.* **1993**, 93, 105.

(22) Zanella, R.; Giorgio, S.; Henry, C. R.; Louis, C. *J. Phys. Chem. B* **2002**, 106, 7634.

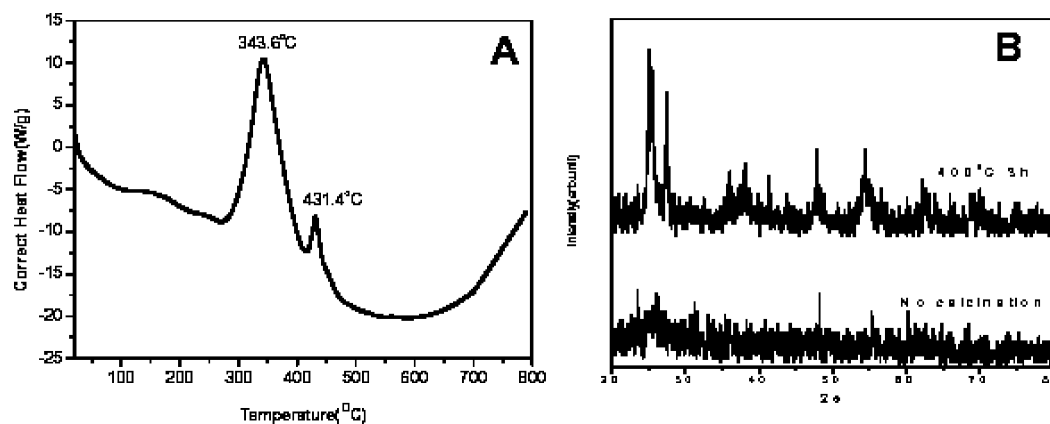


Figure 3. (A) DSC curve of the as-prepared 1-D TiO_2 -OLA and (B) the XRD diffraction patterns of the as-prepared and the calcined TiO_2 -OLA.

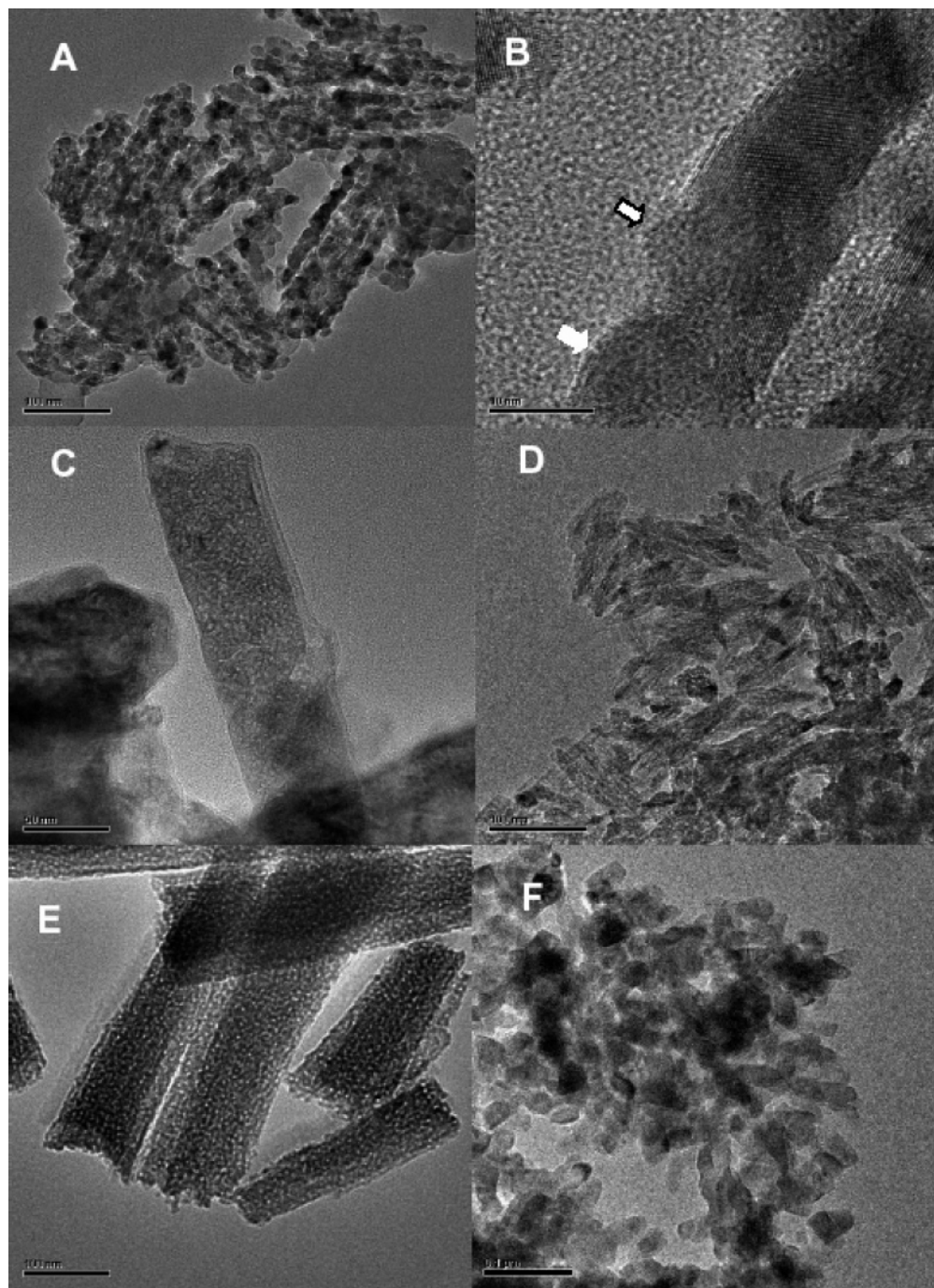


Figure 4. Stability of the 1-D TiO_2 nanostructures against sintering. TEM images of TiO_2 -AL (A and B), TiO_2 -OLA (C), and TiO_2 -IBA (D) after calcination at 400 °C for 2 h. E and F are TiO_2 -OLA calcined at 300 and 600 °C, respectively.

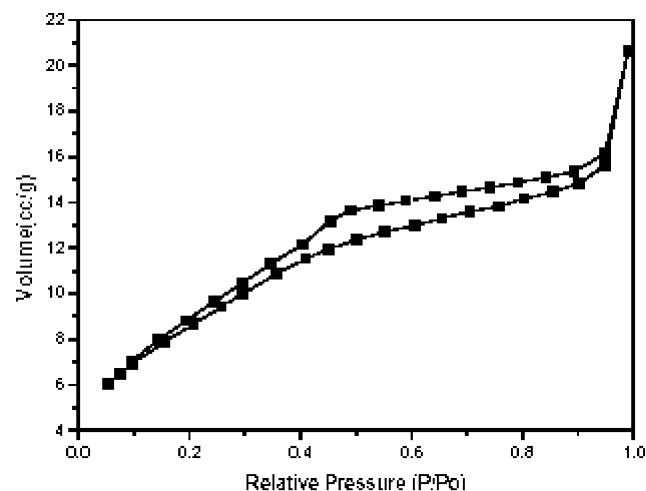


Figure 5. Nitrogen adsorption/desorption isotherm of TiO_2 -OLA calcined at 300 °C for 2 h.

in a range of textures after calcination implies more than one possible formation mechanism. It is well documented that alkylamines can be selectively adsorbed on certain crystal facets of metal oxides or form amine adducts of titanium tetra-alkoxides,^{18c} thus lead to orientated growth or aggregation of metal oxide particles.^{14,16,18a,b} After the removal of alkylamines, porous texture in the middle and a thick wall are left in this case. For aniline, the presence of a highly hydrophobic benzyl group may instead result in the formation of reverse micelles in the solution. Namely, the aniline molecules surrounded the water drop that was formed in its center. These micelles may then act as “soft templates” to confine further reaction within the micelle region but still lead ultimately to the formation of 1-D structures, probably via self-assembly from multiply charged polyanate anions.^{14a} The existence of carboxylic acids may also slow the hydrolysis rate of titanium alkoxides because they can replace alcoholic groups¹⁶ or can coordinate to titania gel.²¹ As mentioned above, the slowing down of the hydrolysis step is important to the unidirectional growth of TiO_2 .

TiO_2 -supported Au catalysts have been under intense scrutiny since the original report of their exceptionally high CO oxidation activities at low-temperature,² when Au is

supported on the 1-D TiO_2 nanomaterials (parts A and B of Figure 6). Here TiO_2 -OLA was used as catalyst support, which was calcined at 300 °C for 2 h prior to the catalyst preparation by deposition precipitation²²). Preliminary tests in a microtubular flow reactor indicate that the catalyst has good activity at low temperatures. With an Au loading as low as 1.0 wt % and a GHSV of 15 000 mL/h g catalyst, a stream of 1% CO in air is completely converted to CO_2 below 40 °C, while for catalyst of 1% Au supported on commercial TiO_2 (TiO_2 from Aldrich, Anatase, surface area 50 m^2/g), the complete CO conversion temperature is 90 °C.

In summary, we report a novel one-pot method for the preparation of 1-D and porous TiO_2 nanostructures. Coupling the hydrolysis of titanium isopropoxide with esterification (2-propanol/acetic acid as “controlled-release” water supply) and by partial substitution of alcoholic groups by carboxylic acids in titanium alkoxide, surfactant guided unidirectional growth is simply realized in a one-pot process. The amount, and release rate, of water can be tuned by changing reaction temperature and molar ratio of the esterification reactants. In this way, the hydrolysis and condensation steps are effectively separated and directional growth can be obtained. By use of octylamine, isobutylamine, and aniline as growth-directing agents, 1-D TiO_2 nanostructures can be prepared in a range of dimensions, aspect ratios, and textures. These as-prepared 1-D nanostructures are poorly crystallized, but well-developed anatase phase structure is obtained above 400 °C, and rutile phase was detected above 800 °C. For octylamine and isobutylamine, the nanofibers are probably formed via orientated growth mechanism, while for aniline, a micelle-related mechanism for formation of organo-titanate species and subsequent self-assembly into 1-D nanostructures seems more likely. Preliminary results show that Au supported on these TiO_2 nanofibers has high catalytic activity for CO oxidation at near ambient temperature with low Au loading.

Acknowledgment. The research was supported by Agency for Science, Technology and Research in Singapore. We thank Drs. Keith Carpenter and P. K. Wong for support of this project and Dr. James Highfield, Ms. Alamelu Suriya Subramani, and Mr. Weiqiang Lim for technical assistance.

CM051695B

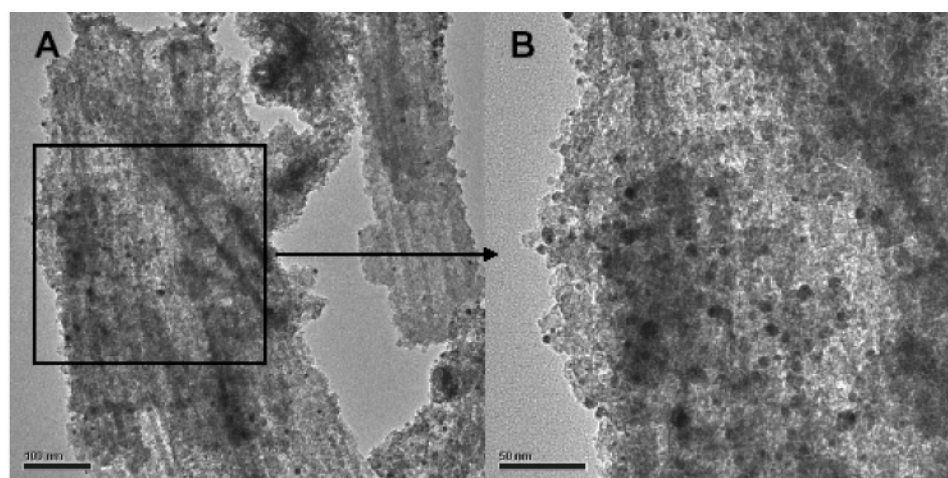


Figure 6. TEM images of the prepared Au/ TiO_2 -OLA catalyst. The black dots are Au particles. A selected area in image A is magnified to provide image B.